Macromolecular Research, Vol. 12, No. 2, pp 189-194 (2004)

Reorientation of Colloidal Crystalline Domains by a Thinning Meniscus

Sang Hyuk Im and O Ok Park*

Department of Chemical & Biomolecular Engineering, Korea Advanced Institute of Science and Technology, 373-1 Guseong, Yuseong, Daejeon 305-701, Korea

Moo Hyun Kwon

Department of Chemical Engineering, Woosuk University, 490 Hujung, Samrae, Wanju, Jeonbuk 656-701, Korea

Received August 7, 2003; Revised February 18, 2004

Abstract: When water is evaporated quickly from a water-based colloidal suspension, colloidal particles protrude from the water surface, distorting it and generating lateral capillary forces between the colloidal particles. The protruded colloidal particles are then assembled into ordered colloidal crystalline domains that float on the water surface on account of their having a lower effective density than water. These colloidal crystal domains then assemble together by lateral capillary force and convective flow; the generated colloidal crystal has grain boundaries. The single domain size of the colloidal crystal could be controlled, to some extent, by changing the rate of water evaporation, but it seems very difficult to fabricate a single crystal over a large area of the water's surface without reorienting each colloidal crystal domain. To reorient such colloidal crystal domains, a glass plate was dipped into the colloidal suspension at a tilted angle because the meniscus (airwaterglass plate interface) is pinned and thinned by further water evaporation. The thinning meniscus generated a shear force and reoriented the colloidal crystalline domains into a single domain.

Keywords: colloidal crystals, colloidal suspension, contact line, photonic bandgap, single crystal.

Introduction

Synthesis of three-dimensional (3D) periodic structures through colloidal crystal templating is a topic receiving increased attention in the field of materials chemistry due to the potential applications of these structures in confining and controlling light in all three directions of space. These 3D regular structures, called photonic bandgap (PBG) crystals, can be used as lasers,[1] waveguides,[2] chemical sensors,[3] and optical filters.[4] Accordingly, intensive studies on the fabrication of such 3D PBG crystals have been performed for last decades. In particular, colloidal PBG crystals using mono-dispersed colloidal particles have considerable attraction due to their relative easy processes and cost effectiveness compared to the conventional microfabrication techniques. In the fabrication of the large single crystalline colloidal the PBG crystals, maintaining a low defect density is of great importance because the optical properties of the PBG crystals are closely related to such defects. Generally, colloidal crystals have been made by the gravitational sedimentation,[5] electrophoresis,[6] vertical deposition,[7] vertical deposition with temperature gradient,[8] and colloidal assembly on a water surface.[9] Making a single colloidal crystal through the methods of sedimentation and electrophoresis is difficult because such methods form polycrystalline domains unless colloidal particles are assembled onto a patterned plate, confining colloidal particles. The vertical deposition method seems to provide one route to the formation of a single colloidal crystal. This method involves the assembling of colloidal particles at a water-air-glass plate interface. In a previous study, we reported a method assembling colloidal particles at a water-air interface.[9] In this paper, we focused on what types of colloidal crystals, single or polycrystalline, are assembled at a water-air interface and examined how the assembled colloidal crystal domains on the water surface were reoriented by a thinning meniscus.

Experimental

Preparation of PS Colloidal Particles. PS submicron-sized particles were synthesized by emulsifier-free emulsion polymerization.[10-14] Deionized water (450 g) was poured into a reactor and the water was kept at a temperature of 80 °C

*e-mail: ookpark@webmail.kaist.ac.kr

and stirred at 350 rpm. Sodium styrene sulfonate (0.08 g) as an emulsifier and sodium hydrogen carbonate (0.25 g) as a buffer were inserted into the water. After 10 min, styrene monomer (50 g) was inserted into the solution. After 1 h, potassium persulfate (0.25 g) was introduced into the solution. Finally, polymerization was performed under a nitrogen atmosphere for 18 h.

The effective diameter of the prepared PS colloidal particles measured by a light scattering (Zeta Plus, Brookhaven Instrument Corp.) was 450 nm, and their polydispersity was 0.005. The values are averages of the five measurements. The diameter of the corresponding PS colloids measured by scanning electron microscopy (SEM) was 440 nm.

Colloidal Crystal Fabrication Procedures.

Without Reoriented Colloidal Crystals: Wettable tape (2.5×2.5 cm^2) was attached to three of the glass plate to create a concave suspension interface within which the colloidal suspension (water medium) could be confined. Then, 100 μL of the 5 wt% PS (440 nm in diameter) colloidal suspension was dropped onto each glass plate. The glass plates were placed in a humidity-controlled furnace at 60 °C in order to assemble the colloidal particle three-dimensionally through the water evaporation. To examine effect of the evaporation rate of water on the colloidal crystalline domains, water was evaporated at a rate of 10, 1.7, and 0.4 μL/min, respectively.

Reoriented Colloidal Crystals: Two glass plates were dipped at a tilted angle of 10° with respect to the vertical into 1 wt% PS colloidal suspensions (40 mL) contained in Pyrex beakers (50 mL, diameter = 4 cm), respectively. Water in the suspensions was evaporated at a rate of 2 and 0.7 mL/h in a furnace of 60 °C.

Results and Discussion

First, three-dimensional colloidal crystal was fabricated by the water evaporation method[9] as described in Figure 1. Water was evaporated at a rate of 10 μL/min (a fast water evaporation rate). The resulting SEM surface and cross-sectional images were shown in Figure 3(a) and (d), respectively. Figure 3(a) shows that the colloidal crystal has multiple domains, which are separated from each other by grain boundaries. The magnified image of Figure 3(a) clearly shows that the assembled colloidal crystal is not a single crystal. Each colloidal crystal grain also reveals that the colloidal particles assemble into a face centered cubic (FCC) structure and the (111) planes of the FCC structure are oriented parallel to the plate (see the magnified image and cross-sectional image (Figure 3(d)). In addition, this provides important evidence that each grain preferentially formed on the water surface and then assembled. The reason is schematically illustrated in Figure 2. When the colloidal suspension is confined by the wettable wall, the interface of the suspension becomes concave as depicted in Figure 2(a).

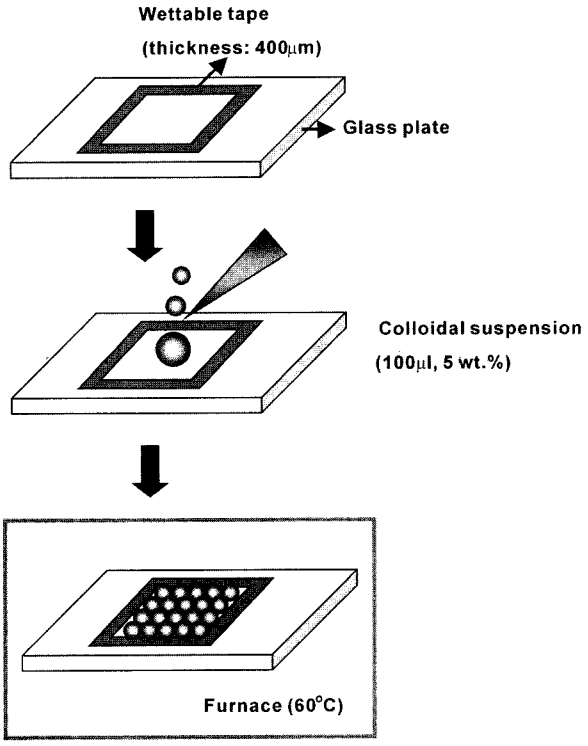

Figure 1. Fabrication scheme of three-dimensional colloidal crystal through water evaporation method.

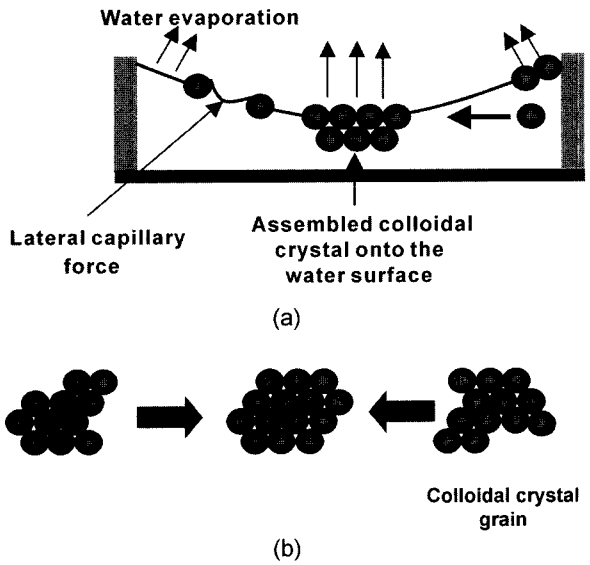

Figure 2. Schematic illustration of colloidal self assembly on a water surface; (a) side view and (b) top view.

The protruding particles from the water surface, caused by the instantaneous water evaporation, distort the suspension interface and assemble into an ordered microstructure by lateral capillary force,[15-19] which is generated by the dis-

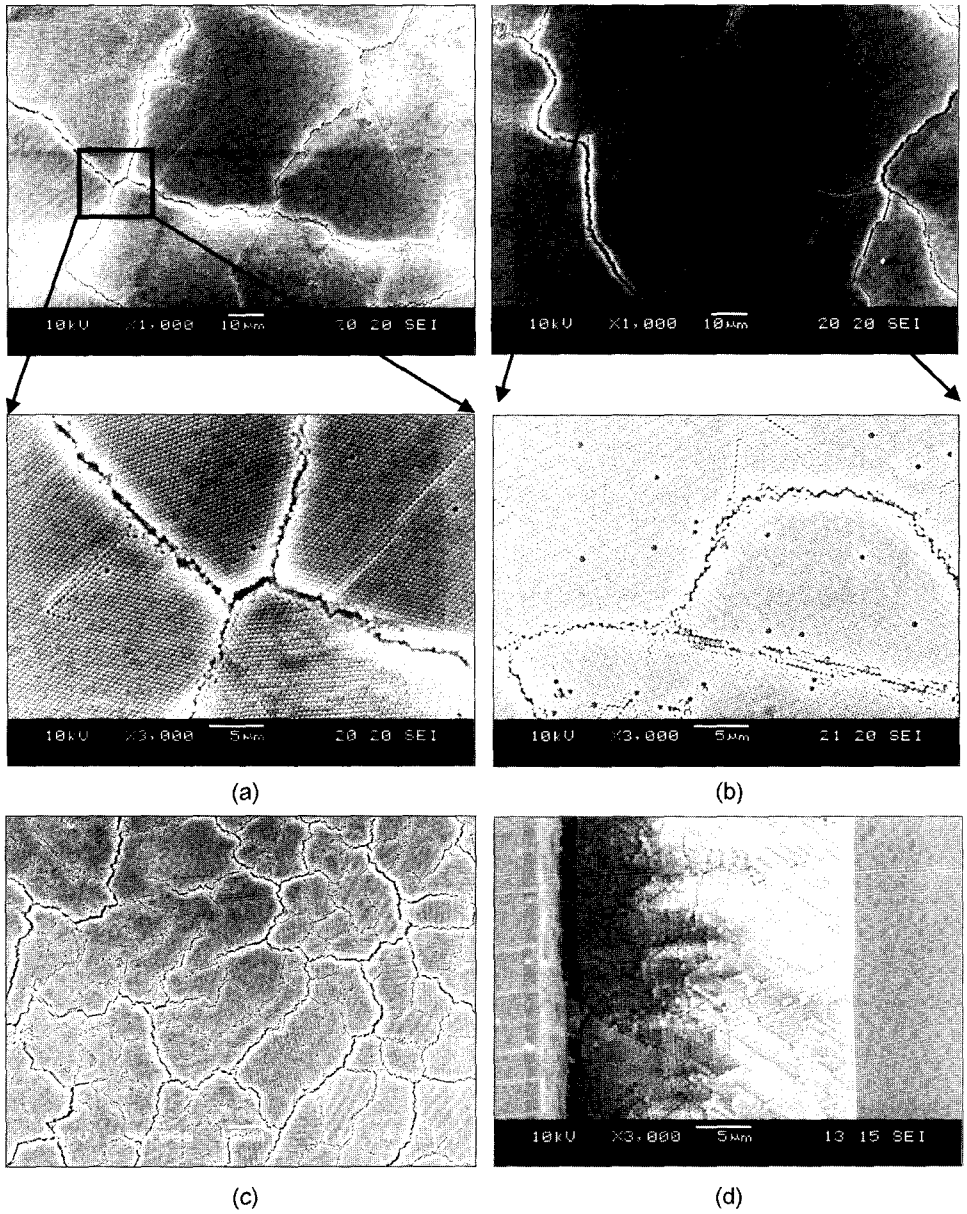

Figure 3. SEM surface images of generated colloidal crystals with water-evaporation rate. (a) 10 μL/min, (b) 1.7 μL/min, (c) 0.4 μL/min, and (d) its representative cross-sectional image.

torted interface between protruding colloidal particles. The ordered microstructure (one colloidal crystal grain) floats on the water surface because its effective density becomes smaller than water density.[9] The microstructures are also assembled together by the lateral capillary force and the convective flow (see Figure 2(b)). In the end, colloidal crystals have polycrystalline domains because nucleation of colloidal particle on the surface tends to occur concurrently at many locations. It seems that the colloidal crystal cannot help but having grain boundaries as the colloidal crystalline domains do not reorientate.

To examine how the water evaporation rate affects the domain size of the colloidal crystal, we controlled the evaporation rate. When water was evaporated at a rate of 1.7 μL/min (medium water evaporation rate), a SEM surface image of the resulting colloidal crystal is shown in Figure 3(b). The average size of the single colloidal crystal domain was over $100 \times 100\ \mu m^2$ while that obtained under the fast water evaporation rate condition was about $50 \times 50\ \mu m^2$. When the water evaporation rate is reduced, the possibility of nucleation of the colloidal particles on the water surface is diminished and convective flow caused by the water evaporation becomes weak. The reduced nucleation site provides colloidal particles to the wider spatiality assembling on the

water surface and the weakened convective flow gives the colloidal crystalline much more growing time because each growing colloidal crystalline are assembled by the convective flow and thus weakened convective flow moves and assembles colloidal crystalline domains slowly. Accordingly, the resulting colloidal crystal has a larger single crystal domain than the colloidal crystal obtained under the fast water evaporation rate condition. This shows that the size of the single colloidal crystal domain can be controlled some content changing the water evaporation rate. However the colloidal crystal still has grain boundaries. The magnified image in Figure 3(b) reveals such grain boundaries. When the water evaporation rate is further reduced, at a rate of 0.4 μL/min (slow water evaporation rate), a SEM surface image of the resulting colloidal crystal is shown in Figure 3(c) (ordered region). The colloidal crystal reveals an ordered region and a disordered region. This image shows that colloidal particles assemble into the smaller domain and have many defects (line and point defects). This may be because a very slow water evaporation rate provides colloidal particles to few chances to protrude from the water surface. Accordingly, the number of nucleation sites on the water surface are dramatically reduced. In addition, the assembled colloidal crystals on the water surface cannot grow larger because few colloidal particles protrude from the water surface, distorting the water surface and generating the lateral capillary force that assembles colloidal particles. Very weakened convective flow cannot assemble each colloidal crystal grain tightly. Colloidal particles that do not protrude from the water surface and that do not assemble into ordered microstructures settle to the glass plate because the density of each colloidal particle (1.04 g/cm^3) is larger than that of water (1 g/cm^3). These settled colloidal particles form disordered regions. Therefore, the colloidal crystal grains have smaller domains and many defects. In summary, a single colloidal crystal domain can be enlarged to some extent by changing the water evaporation rate, but it seems to be very difficult for colloidal particles to assemble into a single crystal over a large area without applying any external driving force to reorient each colloidal crystal grain.

When a wettable plate (a glass or silicon plate) is dipped into a colloidal suspension (water medium) at a tilted angle, colloidal particles are pinned at the glass-water-air interface (meniscus edge) by water evaporation. The pinned colloidal particles fix the meniscus edge, although the height level of the suspension decreases by further water evaporation. Accordingly, the meniscus shape is extended and becomes steep.[14] These phenomena are expected to reorient colloidal crystal grains because the extended meniscus generates shear force. Therefore, we dipped a glass plate at a tilted angle of 10° with respect to the vertical into a 1 wt% PS colloidal suspension (40 mL) contained in Pyrex beaker (50 mL, diameter = 4 cm). Water in the suspension evaporated at a rate of 2 mL/h in a furnace of 60 °C. Colloidal particles were then assembled on the water surface as depicted in Figure 2. The colloidal crystals formed on the water surface revealed grain boundaries. As water evaporated, colloidal particles were assembled and pinned along the glass-water-air interface (meniscus edge). Water evaporation plays an important role in moving not only colloidal particles but also the assembled colloidal crystal grains toward the meniscus edge. Further water evaporation induces the meniscus shape steep generating shear force.[14] The resulting SEM surface image is shown in Figure 4. This shows that each colloidal crystal grain is reoriented by the thinning meniscus and some colloidal particles are confined between such grains. Generally, in colloidal crystals, colloidal particles assemble into an FCC structure and the (111) planes of FCC structure are oriented parallel to the plate (see SEM surface images of Figures 3 and 5). Each colloidal crystal grain showed such a tendency. Colloidal particles confined between colloidal crystal grains reveal that the (100) planes of FCC structure are oriented parallel to the plate. This is caused by the colloidal crystal grains not having sufficient time to reorient into a single crystal due to fast water evaporation rate. Therefore, we repeated the above experiment with a water evaporation rate of 0.7 mL/h. The resulting SEM surface image is shown in Figure 5(a). This clearly shows that the colloidal particles are assembled into a single crystal because this crystal does not reveal any grain boundaries over whole areas. The cracks appearing on the crystal were generated by the electron beam damage of SEM setup or drying process. Its cross-sectional SEM image (Figure 5(c)) also shows that the colloidal particles are assembled into a single crystal without disordered regions from bottom to top.

Photographs of colloidal crystals having multiple colloidal crystal domains and single crystal domains are shown in Figure 6(a) and (b), respectively. Polycrystalline colloidal crystal, as anticipated in Figure 3, showed various brilliant opalescent colors because each crystal domain reflects light

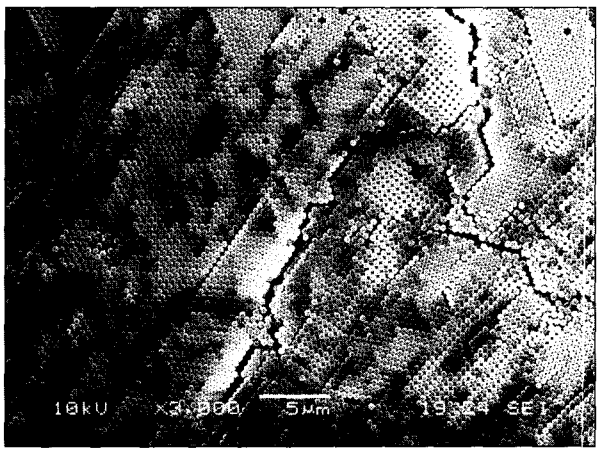

Figure 4. SEM surface image of reoriented colloidal crystal domains (water evaporation rate = 2 mL/h).

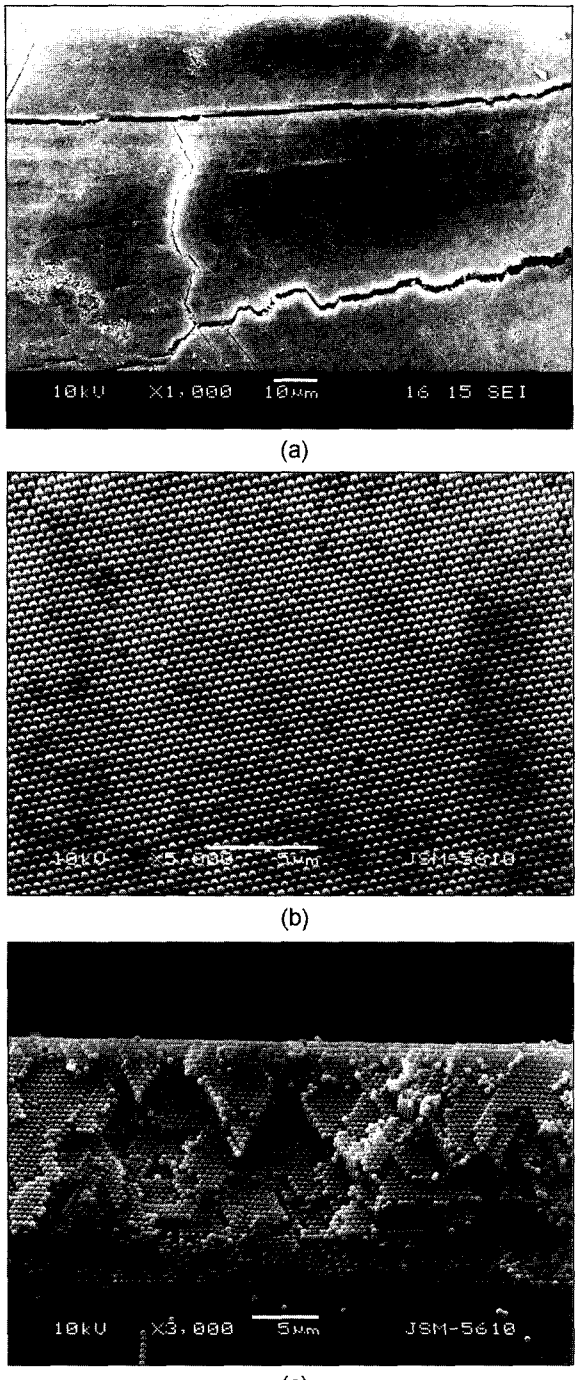

Figure 5. SEM surface images of (a) reoriented colloidal crystal domains (water evaporation rate = 0.7 mL/h), (b) its magnified image, and (c) cross-sectional image.

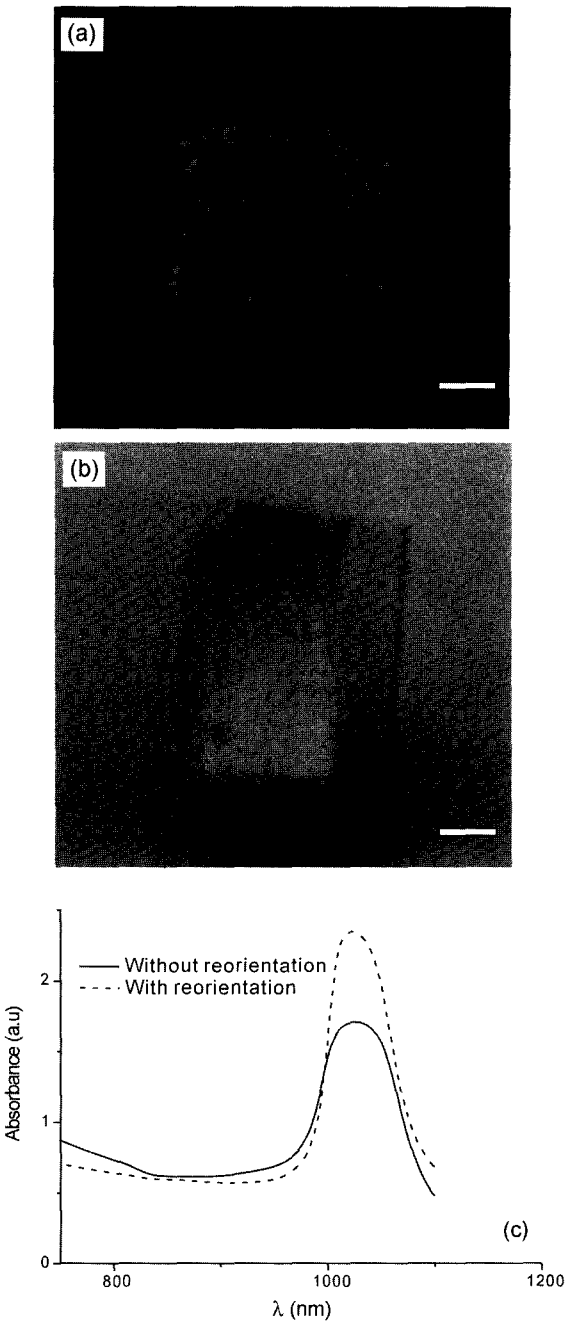

Figure 6. Photographs of colloidal crystals having (a) multiple colloidal crystal domains, (b) single crystal domain, and (c) UV-VIS absorption spectra. The scale bar is 0.5 cm.

of different wavelengths. On the other hand, single colloidal crystals, as expected in Figure 5, showed homogeneous iridescent colors. These figures provide indirect evidence that colloidal crystals are assembled into a single crystalline or a polycrystalline structure. The transmission spectra of the colloidal crystals can represent colloidal crystal states because the presence of the defects in colloidal crystals affects the photonic bandtail states and, thus, enhances the transmission in the gap.[20] The absorption spectra (see Figure 6(c)) were measured by ultraviolet-visible (UV-VIS) spectroscopy because PS colloids show a little absorption in the visible region and, consequently, can represent the transmission spectra. This absorption spectra show that a single colloidal

crystal has deeper photonic stop bandgap and narrower stop bandwidth than does a polycrystalline colloidal crystal because the colloidal crystal domains act like defects.

Conclusions

In a water based-colloidal suspension, when water is evaporated fast, the colloidal particles protrude from the water surface and form ordered colloidal crystal domains on the water surface. Such colloidal crystal domains are assembled together by the lateral capillary force and convective flow, having colloidal crystalline domain boundaries. The single colloidal crystalline domain size could be controlled to some extent by changing the water evaporation rate. However, it was very difficult to fabricate a single colloidal crystal over a large area on the water surface without reorienting such colloidal crystal domains. The colloidal crystalline domains could be reoriented by the shear force generated from thinning meniscus.

Acknowledgements. The authors are grateful to the Center for Advanced Functional Polymers, which is supported by KOSEF. This work was also partially supported by the Brain Korea 21 Project

References

(1) M. N. Shkunov, X. V. Vardeny, M. C. DeLong, R. C. Poloson, A. A. Zakhidov, and R. H. Baughman, *Adv. Funct. Mater.*, **12**, 21 (2002).
(2) L. Vogelaar, W. Nijda, H. A. van Wolferen, R. M. de Ridder, F. B. Segerink, E. F. L. Kuipers, and N. F. van Hulst, *Adv. Mater.*, **13**, 1551 (2001).
(3) K. Lee and S. A. Asher, *J. Am. Chem. Soc.*, **122**, 9534 (2000).
(4) S. H. Park and Y. Xia, *Langmuir*, **15**, 266 (1999).
(5) H. Miguez, F. Meseguer, C. Lopez, A. Blanco, J. Moya, J. requena, A. Mifsud, and V. Fornes, *Adv. Mater.*, **10**, 480 (1998).
(6) A. L. Rogach, N. A. Kotov, D. S. Koktysh, J. W. Ostrander, and G. A. Ragoisha, *Chem. Mater.*, **12**, 2721 (2000).
(7) P. Jiang, J. F. Bertone, K. S. Hwang, and V. L. Colvin, *Chem. Mater.*, **11**, 2132 (1999).
(8) Y. A. Vlasov, X.-Z. Bo, J. C. Sturm, and D. J. Norris, *Nature*, **414**, 289 (2001).
(9) S. H. Im, Y. T. Lim, D. J. Suh, and O. O. Park, *Adv. Mater.*, **14**, 1367 (2002).
(10) G. R. Yi, J. H. Moon, and S.-M. Yang, *Chem. Mater.*, **13**, 2613 (2001).
(11) J. H. Kim, M. Chainey, M. S. El-Aasser, and J. W. Vanderhoff, *J. Polym. Sci., Polym. Chem.*, **30**, 171 (1992).
(12) K. Chengyou, L. Huihui, and Y. Qing, *Korea Polym. J.*, **5**, 221 (1997).
(13) M. S. Park, *Korea Polym. J.*, **2**, 54 (1994).
(14) S. H. Im, O. O. Park, and M. H. Kwon, *Macromol. Res.*, **11**, 110 (2003).
(15) N. D. Denkov, O. D. Velev, P. A. Kralchevsky, I. B. Ivanov, H. Yoshimura, and K. Nagayama, *Nature*, **361**, 26 (1993).
(16) N. D. Denkov, O. D. Velev, P. A. Kralchevsky, I. B. Ivanov, H. Yoshimura, and K. Nagayama, *Langmuir*, **8**, 3183 (1992).
(17) E. Adachi, A. S. Dimitrov, and K. Nagayama, *Langmuir*, **11**, 1057 (1995).
(18) A. S. Dimitrov and K. Nagayama, *Langmuir*, **12**, 1303 (1996).
(19) M. Yamaki, J. Higo, and K. Nagayama, *Langmuir*, **11**, 2975 (1995).
(20) Y. H. Ye, F. LeBlanc, A. Hache, and V. V. Truong, *Appl. Phys. Lett.*, **78**, 52 (2001).